Multimedia Tools and Applications (2019) 78:18095–18112
https://doi.org/10.1007/s11042-019-7170-y

An adaptive second-order partial differential equation based on TV equation and *p*-Laplacian equation for image denoising

Xiaojuan Zhang[1,2] · **Wanzhou Ye**[1]

Received: 19 March 2018 / Revised: 22 November 2018 / Accepted: 3 January 2019 /
Published online: 19 January 2019

Abstract
This paper introduces an adaptive diffusion partial differential equation (PDE) for noise removal, which combines a total variation (TV) term and a p-Laplacian ($1 < p \leq 2$) term. Utilizing the edge indicator, we can adaptively control the diffusion model, which alternates between the TV and the p-Laplacian($1 < p \leq 2$) in accordance with the image feature. The main advantage of the proposed model is able to alleviate the staircase effect in smooth regions and preserve edges while removing the noise. The existence of a weak solution of the proposed model is proved. Experimental results confirm the performance of the proposed method with regard to peak signal-to-noise ratio (PSNR), mean structural similarity (MSSIM) and visual quality.

Keywords Image denoising · TV · p-Laplacian · Adaptive equation · Weak solution

1 Introduction

Image denoising is an important step in low-level image processing and computer vision. Image denoising aims to preserve important structure features including edges and corners while removing the noise in the image. The variational [4, 6, 8, 11, 12, 16, 19] and partial differential equations (PDEs) [9, 10, 13–15, 18, 23] based methods are very popular for removing noise during the last two decades [3]. Despite the success enjoyed by these methods, there are problems related to fine structure and edge preservation, staircase effect or over-smoothing of images.

✉ Wanzhou Ye
wzhy@shu.edu.cn

Xiaojuan Zhang
zhangxiaojuan@ncwu.edu.cn

[1] Department of Mathematics College of Science, Shanghai University, Shanghai, China

[2] School of Mathematics and Statistics Science, North China University of Water Resources and Electric Power, Zhengzhou, China

Consider the following representative minimization problem

$$\min_u E(u) = \frac{1}{p}\int_\Omega |\nabla u|^p dx, \tag{1}$$

where the minimizer u is the restored image, $\Omega \subset \mathbb{R}^2$ is the image domain with $1 \le p \le 2$. The formal gradient flow associated with the functional E(u) is given by,

$$\frac{\partial u}{\partial t} = \mathrm{div}(|\nabla u|^{p-2}\nabla u), \tag{2}$$

when $p = 1$, it is the widely used total variation (TV) based scheme proposed in 1992 [16]. In [6], the existence and uniqueness of TV minimization was proved in the space of functions of bounded variation (BV), and the corresponding gradient flow was treated in [1, 2]. The TV-based model performs better at preserving edge sharpness and location while removing noise but creates patchy or staircase effect within homogeneous, smooth or moderate gradient regions [7]. Choosing $p = 2$ results in isotropic diffusion, which removes the noise and solves the staircase problem but is at the expense of edge blurring. Taking a fixed value $1 < p < 2$ results in an anisotropic diffusion, which is somewhere between TV model and isotropic smoothing. However, there is a trade-off between edge preservation and piecewise smooth regions reconstruction.

In order to mitigating the drawbacks of TV-based and isotropic diffusion, various remedies have been proposed [6, 8, 12, 24]. For instance, Chamboll and Lions [6] proposed minimizing the following energy functional, which combines TV-based and isotropic diffusion

$$\min_{u\in BV(\Omega)} E(u) = \frac{1}{2\beta}\int_{|\nabla u|\le\beta} |\nabla u|^2 dx + \int_{|\nabla u|\ge\beta} |\nabla u| - \frac{\beta}{2} dx. \tag{3}$$

Here β is a fixed positive number and it is a threshold of $|\nabla u|$. As $|\nabla u| \le \beta$, it means isotropic diffusion. As $|\nabla u| \ge \beta$, the TV energy is used. This model is successful in restoring images in which homogeneous regions are separated by distinct edges. However, this model is closely linked to β and a fixed threshold can lead to bad results [8, 24]. In order to solve this problem, Zhou et al. [24] introduced a locally adaptive version of the model (3):

$$\min_u E(u) = \frac{1}{2\beta(x)}\int_{|\nabla u|\le\beta(x)} |\nabla u|^2 dx + \int_{|\nabla u|\ge\beta(x)} |\nabla u| - \frac{\beta(x)}{2} dx, \tag{4}$$

where the adaptive parameter $\beta(x)$ is obtained by solving a separate energy minimization problem. This model can remove noise while preserve the edge. However, Zhou [24] lacks a strong theoretical foundation.

Recently, motivated by the correspondence between the variational and PDE methods for imaging problems, Surya Prasath et al. [18] proposed adaptive forward-backward diffusion equation (AFBD for short) of the following form:

$$\frac{\partial u}{\partial t} = \mathrm{div}\left(h(\nabla G_\sigma * u)|\nabla u|^{p-2}\nabla u\right), \tag{5}$$

where $p \ge 1$. $h(\nabla G_\sigma * u)$ is an edge detector and given by,

$$h(\nabla G_\sigma * u) = \frac{1}{1 + k|\nabla G_\sigma * u|^2}, \tag{6}$$

where $k > 0$. G_σ denotes the two-dimensional Gaussian kernel $G_\sigma = (2\pi\sigma)^{-1}\exp(-|x|^2/2\sigma^2)$, $\sigma > 0$ is a constant. The authors proved the existence of weak solutions for (5). As $p = 1$, their experimental results showed that their model overcome well-known edge smearing effects of the heat equation by using gradient dependent diffusion function.

However, the resulting image in the presence of the noise also showed staircase effect. When $p > 1$ (for example $p = 1.5$, see Section 3 Figs. 3g, 4g, 5h), the model (5) alleviates the staircase effect but dose not preserve the edge.

In order to alleviate the staircase effect in smooth regions and preserve edges while removing the noise, we propose a novel adaptive PDE model based on TV equation and p-Laplacian equation. Our proposed model can have the following form

$$\frac{\partial u}{\partial t} = \operatorname{div}\left(h(\nabla G_\sigma * u)|\nabla u|^{p-2}\nabla u + \mu(1 - h(\nabla G_\sigma * u))\frac{\nabla u}{|\nabla u|}\right), \tag{7}$$

where $1 < p \leq 2$, $\mu > 0$ is a constant.

Now let us mention the advantage of the proposed model. Firstly, the proposed model joints TV term which is edge preserving and p-Laplacian ($1 < p \leq 2$) term which helps in effective noise removal. In homogeneous regions, we make use of the p-Laplacian term to reduce the noise and avoid the staircase effect; and near edges, we utilize the TV term to preserve them. By using the edge indicator $h(\nabla G_\sigma * u)$, we roughly segment the image into two subregions, i.e., the homogeneous regions and the region's nearby boundaries. In the homogeneous regions, the magnitude of $|\nabla G_\sigma * u|$ is small, thus the edge detector function $h(\nabla G_\sigma * u)$ is close to one, so the proposed model acts as the p-Laplacian equation ($1 < p \leq 2$) to remove the noise and alleviate the staircase effect; in the region's nearby boundaries, the magnitude of $|\nabla G_\sigma * u|$ is large, then the edge detector function $h(\nabla G_\sigma * u)$ takes smaller value (close to zero), so the proposed model acts as the TV diffusion equation to preserve the edge. Secondly, in contrast to the previous anisotropic diffusion PDEs, we prove the existence of a weak solution of the proposed equation, which is very important for the numerical computation. Thirdly, experimental results on different noisy images indicate the advantage of the proposed adaptive model. The proposed approach is proven to provide better edge preserving with effective noise removal both theoretically and illustrated experimentally using a variety of example.

The rest of the paper is organized as follows. In Section 2, we give some important lemmas and then prove the existence of a weak solution of the proposed problem. Section 3 details the numerical aspects and shows comparison denoising results on noisy images. Finally, Section 4 concludes the paper.

2 Existence of weak solutions

The problem (7) is complemented with the initial condition

$$u(x, 0) = u_0, \tag{8}$$

and boundary condition

$$\frac{\partial u}{\partial \boldsymbol{n}} = 0, \tag{9}$$

where $\boldsymbol{n} = (n_1, n_2)$ is the outward normal direction on $\partial\Omega$, In this section, we establish the existence of a weak solution of the proposed model (7), (8) and (9).

2.1 Weak solutions and the main result

The symbol $\|\cdot\|$ will stand for the Euclidean norm in $L^2(\Omega)$. The corresponding scalar product will be denoted by parentheses $(\cdot, \cdot)$. We will also use this notation for duality between $L^p(\Omega)$ and $L^{p/p-1}(\Omega)$. The symbols $C(\mathcal{J}; E)$, $C_w(\mathcal{J}; E)$, $L^2(\mathcal{J}, E)$ etc denote

the spaces of continuous, weakly continuous, quadratically integrable etc functions on an interval $\mathcal{J} \subset \mathbb{R}$ with values in a Banach space E.

Definition 1 A function u from the class

$$u \in C_w\left(0,T;L^2(\Omega)\right)\bigcap L^p(0,T;W^{1,p}(\Omega))\bigcap W^{1,p/(p-1)}\left(0,T;\left[L^2\bigcap W^{1,p}(\Omega)\right]^*\right) \tag{10}$$

is called a weak solution to problems (7), (8) and (9) with $u_0 \in L^2(\Omega)$,
if

(i) there exists $z \in L^\infty(\Omega \times (0,T);\mathbb{R}^2)$, $\|z\|_{L^\infty(\Omega\times(0,T);\mathbb{R}^2)} \le 1$, so that for all $v \in L^2 \cap W^{1,p}(\Omega)$,

$$\left\langle \frac{du}{dt}, v\right\rangle + (h(\nabla G_\sigma * u)|\nabla u|^{p-2}\nabla u, \nabla v) + \mu((1-h(\nabla G_\sigma * u))Z, \nabla v) = 0 \tag{11}$$

a.e. on (0,T);

(ii) for all $w \in L^p(0,T;W^{1,p}(\Omega)) \cap W^{1,1}(0,T;L^2(\Omega))$, one has

$$\begin{aligned}
&\|u(T)-w(T)\|^2 + 2\int_0^T\int_\Omega \frac{dw}{dt}u dxdt\\
&\quad +2\int_0^T\int_\Omega h(\nabla G_\sigma * u)|\nabla u|^p dxdt\\
&\quad +2\mu\int_0^T\int_\Omega (1-h(\nabla G_\sigma * u))|\nabla u| dxdt\\
&\le \|u_0 - w(0)\|^2 + \|w(T)\|^2 - \|w(0)\|^2\\
&\quad +2\int_0^T\int_\Omega h(\nabla G_\sigma * u)|\nabla u|^{p-2}\nabla u\cdot\nabla w dxdt\\
&\quad +2\mu\int_0^T\int_\Omega (1-h(\nabla G_\sigma * u))\, Z\cdot\nabla w dxdt;
\end{aligned} \tag{12}$$

(iii) the initial condition (8) holds in the space $L^2(\Omega)$.

Remark 1 Let us present a motivation for this definition of solution to (7), (8) and (9). Consider a pair (u, Z) of sufficiently smooth functions satisfying (11), (12) and (8). Then, testing (11) by $2(u-w)$ and integrating in time, we deduce

$$\begin{aligned}
&2\int_0^T\int_\Omega \frac{d(u-w)}{dt}\cdot(u-w)dxdt + 2\int_0^T\int_\Omega \frac{dw}{dt}\cdot(u-w)dxdt\\
&+2\int_0^T\int_\Omega h(\nabla G_\sigma * u)|\nabla u|^{p-2}\nabla u\cdot\nabla(u-w)dxdt\\
&+2\mu\int_0^T\int_\Omega (1-h(\nabla G_\sigma * u))\, Z\cdot\nabla(u-w)dxdt = 0.
\end{aligned}$$

we get

$$\begin{aligned}
&\|u(T)-w(T)\|^2+2\int_0^T\int_\Omega \frac{dw}{dt}u dxdt\\
&\quad+2\int_0^T\int_\Omega h(\nabla G_\sigma * u)|\nabla u|^p dxdt\\
&\quad+2\mu\int_0^T\int_\Omega (1-h(\nabla G_\sigma * u))\,|\nabla u| dxdt\\
&=\|u_0-w(0)\|^2+\|w(T)\|^2-\|w(0)\|^2\\
&\quad+2\int_0^T\int_\Omega h(\nabla G_\sigma * u)|\nabla u|^{p-2}\nabla u\cdot\nabla w dxdt\\
&\quad+2\mu\int_0^T\int_\Omega (1-h(\nabla G_\sigma * u))Z\cdot\nabla w dxdt\\
&\quad+2\mu\int_0^T\int_\Omega (1-h(\nabla G_\sigma * u)|\nabla u| dxdt\\
&\quad-2\mu\int_0^T\int_\Omega (1-h(\nabla G_\sigma * u))\,Z\cdot\nabla u dxdt
\end{aligned}$$

Due to (12), we have

$$\int_0^T\int_\Omega (1-h(\nabla G_\sigma * u))\,|\nabla u| dxdt \le \int_0^T\int_\Omega (1-h(\nabla G_\sigma * u))\,Z\cdot\nabla u dxdt.$$

On the other hand,

$$(1-h(\nabla G_\sigma * u))|\nabla u| \ge (1-h(\nabla G_\sigma * u))Z\cdot\nabla u.$$

All these can be true if and only if

$$|\nabla u| = Z\cdot\nabla u$$

i.e.

$$Z=\frac{\nabla u}{|\nabla u|} \tag{13}$$

Substituting (13) into (11) and integrating by parts, we infer

$$\begin{aligned}
&\int_\Omega\left[\frac{\partial u}{\partial t}-\mathrm{div}(h(\nabla G_\sigma * u)|\nabla u|^{p-2}\nabla u)-\mu\mathrm{div}\left((1-h(\nabla G_\sigma * u))\frac{\nabla u}{|\nabla u|}\right)\right]v dx\\
&+\int_{\partial\Omega}\left(h(\nabla G_\sigma * u)|\nabla u|^{p-2}+\mu\frac{1-h(\nabla G_\sigma * u)}{|\nabla u|}\right)\frac{\partial u}{\partial \boldsymbol{n}}v d\mathcal{H}^1=0.
\end{aligned} \tag{14}$$

Testing (14) by any v compactly supported in Ω, we deduce (7). By arbitrariness of v, we deduce

$$\left(h(\nabla G_\sigma * u)|\nabla u|^{p-2}+\mu\frac{1-h(\nabla G_\sigma * u)}{|\nabla u|}\right)\frac{\partial u}{\partial \boldsymbol{n}}=0,\quad \mathcal{H}^1-a.e.\ \text{in}\ \partial\Omega.$$

Since $h(\nabla G_\sigma * u)|\nabla u|^{p-2}+\mu\frac{1-h(\nabla G_\sigma * u)}{|\nabla u|}$ is non-vanishing, the boundary condition (9) is satisfied.

Now we are ready to formulate one of our main result:

Theorem 1 *Let $u_0 \in L^2(\Omega)$. Then there exists a weak solution to (7), (8) and (9) in the class (11).*

2.2 Auxiliary problem

We recall the following abstract observation [20, 25]. Assume that we have two Hilbert spaces, $X \subset Y$, with continuous embedding operator $i : X \to Y$, and $i(X)$ is dense in Y. The adjoint operator $i^* : Y^* \to X^*$ is continuous and, since $i(X)$ is dense in Y, one-to-one. Since i is one-to-one, $i^*(Y^*)$ is dense in X^*, and one may identify Y^* with a dense subspace of X^*. Due to the Riesz representation theorem, one may also identify Y with Y^*. We arrive at the chain of inclusions:

$$X \subset Y \equiv Y^* \subset X^*.$$

Both embeddings here are dense and continuous. Observe that in this situation, for $f \in Y$, $u \in X$, their scalar product in Y coincides with the value of the functional f from X^* on the element $u \in X$:

$$(f, u)_Y = \langle f, u \rangle.$$

Such triples (X, Y, X^*) are called Lions triples.

We will work with the Lions triple $(H^r(\Omega), L^2(\Omega), (H^r(\Omega))^*)$, where $r > 2(p+1)$ is a fixed number. Denote by A the Riesz bijection between the spaces H^r and $(H^r)^*$ (which are not identified).

In order to prove the theorem 1 we first need to study the following auxiliary problem:

$$\begin{cases} \frac{\partial u}{\partial t} + \epsilon A(u) = \operatorname{div}(h(\nabla G_\sigma * u)|\nabla u|^{p-2}\nabla u) + \mu \operatorname{div}\left((1 - h(\nabla G_\sigma * u))\frac{\nabla u}{\epsilon + |\nabla u|}\right), \\ u(x, 0) = u_0, \\ \frac{\partial u}{\partial \boldsymbol{n}} \Big|_{\partial\Omega \times (0,T)} = 0 \,. \end{cases} \tag{15}$$

Here $\epsilon > 0$ is parameter.

The weak form of (15) is the following Cauchy problem, where the first equality is understood in the sense of the space $(H^r)^*$, whereas the second and the third ones are in the sense of space L^2:

$$\frac{du}{dt} + R(u) + \mu Q_\epsilon(u) + \epsilon A(u) = 0, \qquad u \mid_{t=0} = u_0 \,. \tag{16}$$

The operators $R : H^r \to (H^r)^*$ and $Q_\epsilon : H^r \to (H^r)^*$, which respect the boundary condition, are determined by the duality

$$\begin{aligned} \langle R(u), w \rangle &= \left(h(\nabla G_\sigma * u)|\nabla u|^{p-2}\nabla u, \nabla w\right), \\ \langle Q_\epsilon(u), w \rangle &= \left((1 - h(\nabla G_\sigma * u))\frac{\nabla u}{\epsilon + |\nabla u|}, \nabla w\right), \qquad \forall w \in H^r. \end{aligned}$$

We do not use a notation for partial time derivative since we treat (16) as an ODE in a Banach space.

Lemma 1 *Let $u_0 \in L^2(\Omega)$. The Cauchy problem (16) admits a solution u in the class*

$$L^2(0, T; H^r(\Omega)) \cap H^1(0, T; (H^r(\Omega))^*) \cap C([0, T]; L^2(\Omega)). \tag{17}$$

The solution satisfies the following inequality:

$$\begin{aligned}
&\|u(t_*) - w(t_*)\|^2 + 2\int_0^{t_*}\int_\Omega \frac{dw}{dt} u dx dt + 2\int_0^{t_*}\int_\Omega h(\nabla G_\sigma * u)|\nabla u|^p dx dt \\
&\quad + 2\mu\int_0^{t_*}\int_\Omega (1 - h(\nabla G_\sigma * u))|\nabla u| dx dt \\
&\leq \|u_0 - w(0)\|^2 + \|w(t_*)\|^2 - \|w(0)\|^2 + 2\int_0^{t_*}\int_\Omega h(\nabla G_\sigma * u)|\nabla u|^{p-2}\nabla u \cdot \nabla w dx dt \\
&\quad + 2\mu\int_0^{t_*}\int_\Omega (1 - h(\nabla G_\sigma * u))\frac{\nabla u}{\epsilon + |\nabla u|} \cdot \nabla w dx dt \\
&\quad + 2\mu\epsilon\int_0^{t_*}\int_\Omega (1 - h(\nabla G_\sigma * u))\frac{|\nabla u|}{\epsilon + |\nabla u|} dx dt + \frac{\epsilon}{2}\int_0^{t_*}\langle Aw, w\rangle dt, \qquad (18)
\end{aligned}$$

for every $t_* \in [0, T]$ and for every sufficiently regular test function $w : \bar{\Omega} \times [0, T] \to \mathbb{R}$.

Proof □

Note that Ω is bounded, the embeddings $H^r(\Omega) \subset C^1(\bar{\Omega})$ is compact. The operators $R : C^1 \to (H^r)^*$ and $Q_\epsilon : C^1 \to (H^r)^*$ are continuous. Moreover,

$$\begin{aligned}
\|R\|_{(H^r(\Omega))^*} &\leq \|R\|_{(H^1(\Omega))^*} \leq \int_\Omega \left| h(\nabla G_\sigma * u)|\nabla u|^{p-2}\nabla\, u \right| dx \\
&\leq \int_\Omega |\nabla u|^{p-1} dx \leq C\|u\|^p_{C^1(\bar{\Omega})}] \\
\|Q_\epsilon\|_{(H^r(\Omega))^*} &\leq \|Q_\epsilon\|_{(H^1(\Omega))^*} \\
&\leq \int_\Omega \left| (1 - h(\nabla G_\sigma * u))\frac{\nabla u}{\epsilon + |\nabla u|} \right| dx \leq C
\end{aligned}$$

Here, C is independent of ϵ. Therefore, R and $Q_\epsilon : H^r \to (H^r)^*$ are compact operators. These give opportunity to secure existence of solutions to (16) in (17) by an application of the Leray-Schander degree theory (a systematic approach to parabolic problems of kind (16) may be found, e.g., in [25]).

We now fix a sufficiently smooth function $w : \bar{\Omega} \times [0, T] \to \mathbb{R}$. Testing (16) with $2(u - w)$, $0 \leq t_* \leq T$, in the sense of $((H^r)^*, H^r)$ duality, and integrate in time to obtain

$$\begin{aligned}
&\|u(t_*) - w(t_*)\|^2 + 2\int_0^{t_*}\int_\Omega \frac{dw}{dt} u dx dt + 2\int_0^{t_*}\int_\Omega h(\nabla G_\sigma * u)|\nabla u|^p dx dt \\
&\quad + 2\mu\int_0^{t_*}\int_\Omega (1 - h(\nabla G_\sigma * u))\frac{\nabla u}{\epsilon + |\nabla u|} \cdot \nabla u dx dt \\
&= \|u_0 - w(0)\|^2 + \|w(t_*)\|^2 - \|w(0)\|^2 + 2\int_0^{t_*}\int_\Omega h(\nabla G_\sigma * u)|\nabla u|^{p-2}\nabla u \cdot \nabla w dx dt \\
&\quad + 2\mu\int_0^{t_*}\int_\Omega (1 - h(\nabla G_\sigma * u))\frac{\nabla u}{\epsilon + |\nabla u|} \cdot \nabla w dx dt - 2\epsilon\int_0^{t_*}\langle Au, u - w\rangle dt. \qquad (19)
\end{aligned}$$

Note that the following equality holds

$$\int_0^{t_*}\int_\Omega (1-h(\nabla G_\sigma * u))\frac{\nabla u}{\epsilon+|\nabla u|}\cdot\nabla u dxdt = \int_0^{t_*}\int_\Omega (1-h(\nabla G_\sigma * u))|\nabla u| dxdt \\ -\epsilon\int_0^{t_*}\int_\Omega (1-h(\nabla G_\sigma * u))\frac{|\nabla u|}{\epsilon+|\nabla u|}dxdt.$$

An application of Cauchy's inequality yields

$$-2\langle Au, u-w\rangle \le \frac{1}{2}\langle Aw, w\rangle.$$

We derive from (19) that

$$\|u(t_*)-w(t_*)\|^2 + 2\int_0^{t_*}\int_\Omega \frac{dw}{dt}udxdt + 2\int_0^{t_*}\int_\Omega h(\nabla G_\sigma * u)|\nabla u|^p dxdt \\ +2\mu\int_0^{t_*}\int_\Omega (1-h(\nabla G_\sigma * u))|\nabla u| dxdt \\ \le \|u_0-w(0)\|^2 + \|w(t_*)\|^2 - \|w(0)\|^2 + 2\int_0^{t_*}\int_\Omega h(\nabla G_\sigma * u)|\nabla u|^{p-2}\nabla u\cdot\nabla w dxdt \\ +2\mu\int_0^{t_*}\int_\Omega (1-h(\nabla G_\sigma * u))\frac{\nabla u}{\epsilon+|\nabla u|}\cdot\nabla w dxdt \\ +2\mu\epsilon\int_0^{t_*}\int_\Omega (1-h(\nabla G_\sigma * u))\frac{|\nabla u|}{\epsilon+|\nabla u|}dxdt + \frac{\epsilon}{2}\int_0^{t_*}\langle Aw, w\rangle dt.$$

Lemma 2 *Let u be a solution to problem (16), then u satisfies a priori bound*

$$\|u\|_{L^\infty(0,T;L^2(\Omega))} + \|u\|_{L^p(0,T;W^{1,p}(\Omega))} + \|\frac{du}{dt}\|_{L^2(0,T;(H^r(\Omega))^*)} \le C. \tag{20}$$

The constant C is independent of ϵ.

Proof □

Taking $w\equiv 0$ in (19), $0\le t_*\le T$, we derive

$$\|u(t_*)\|^2 + 2\int_0^{t_*}\int_\Omega h(\nabla G_\sigma * u)|\nabla u|^p dxdt \\ +2\mu\int_0^{t_*}\int_\Omega (1-h(\nabla G_\sigma * u))\frac{|\nabla u|^2}{\epsilon+|\nabla u|}dxdt + 2\epsilon\int_0^{t_*}\langle Au, u\rangle dt = \|u_0\|^2.$$

Therefore

$$\|u(t_*)\|^2 \le \|u_0\|^2, \tag{21}$$

$$\int_0^{t_*}\int_\Omega h(\nabla G_\sigma * u)|\nabla u|^p dxdt \le \|u_0\|^2, \tag{22}$$

$$\mu\int_0^{t_*}\int_\Omega (1-h(\nabla G_\sigma * u))\frac{|\nabla u|^2}{\epsilon+|\nabla u|}dxdt \le \|u_0\|^2, \tag{23}$$

$$2\epsilon\int_0^{t_*}\langle Au, u\rangle dt \le \|u_0\|^2. \tag{24}$$

Using (21), we deduce

$$\|u\|_{L^\infty(0,T;L^2(\Omega))} \leq \|u_0\|. \tag{25}$$

Therefore,

$$|\nabla G_\sigma * u| \leq \|\nabla G_\sigma\| \|u\| \leq C\|u\| \leq C. \tag{26}$$

Thus,

$$1 \geq h(\nabla G_\sigma * u) = \frac{1}{1 + k|\nabla G_\sigma * u|^2} \geq C. \tag{27}$$

Using (22), we get

$$C \int_0^{t_*} \int_\Omega |\nabla u|^p dxdt \leq \int_0^{t_*} \int_\Omega h(\nabla G_\sigma * u)|\nabla u|^p dxdt \leq \|u_0\|^2,$$

a.e.

$$\int_0^{t_*} \int_\Omega |\nabla u|^p dxdt \leq C. \tag{28}$$

Using (25), (28) and Lemma 1, we deduce

$$\|u\|_{L^\infty(0,T;L^2(\Omega))} + \|u\|_{L^p(0,T;W^{1,p}(\Omega))} + \|\frac{du}{dt}\|_{L^2(0,T;(H^r(\Omega))^*)} \leq C$$

All the constants C here are ϵ-independent.

2.3 Proof of theorem 1

Proof of Theorem 1 □

Let $\{u_k\}$ be a sequence of solutions (16) with $\epsilon = \epsilon_k$. Set

$$Z_k = \frac{\nabla u_k}{\epsilon_k + |\nabla u_k|}.$$

Then

$$\|Z_k\|_{L^\infty(\Omega \times (0,T);\mathbb{R}^2)} \leq 1. \tag{29}$$

Since (u_k, Z_k) are the solutions to (16) in the sense of Lemma 1, we have

$$\left\langle \frac{du_k}{dt}, v \right\rangle + (h(\nabla G_\sigma * u_k)|\nabla u_k|^{p-2}\nabla u_k, \nabla v) + \mu((1 - h(\nabla G_\sigma * u_k))Z_k, \nabla v) + \epsilon_k \langle Au_k, v\rangle = 0, \tag{30}$$

a.e. on (0,T).

$$\begin{aligned}
&\|u_k(t_*) - w(t_*)\|^2 + 2\int_0^{t_*} \int_\Omega \frac{dw}{dt} u_k dxdt + 2\int_0^{t_*} \int_\Omega h(\nabla G_\sigma * u_k)|\nabla u_k|^p dxdt \\
&\quad + 2\mu \int_0^{t_*} \int_\Omega (1 - h(\nabla G_\sigma * u_k))|\nabla u_k| dxdt \\
&\leq \|u_0 - w(0)\|^2 + \|w(t_*)\|^2 - \|w(0)\|^2 + 2\int_0^{t_*} \int_\Omega h(\nabla G_\sigma * u_k)|\nabla u_k|^{p-2}\nabla u_k \cdot \nabla w dxdt \\
&\quad + 2\mu \int_0^{t_*} \int_\Omega (1 - h(\nabla G_\sigma * u_k))\, Z_k \cdot \nabla w dxdt \\
&\quad + 2\mu\epsilon_k \int_0^t \int_\Omega (1 - h(\nabla G_\sigma * u_k)) \frac{|\nabla u_k|}{\epsilon_k + |\nabla u_k|} dxdt + \frac{\epsilon_k}{2} \int_0^{t_*} \langle Aw, w\rangle dt,
\end{aligned} \tag{31}$$

for all $t^* \in [0, T]$, and

$$u_k(0) = u_0, \tag{32}$$

for all sufficiently smooth function $v, w : \bar{\Omega} \times [0, T] \to \mathbb{R}$.
To prove the theorem, we are going to pass to limit in (30), (31) and (32) as $\epsilon_k \to 0$.

Due to (20) and (29), without loss of generality we have

$$u_k \to u \quad \text{weakly}^* \text{ in } \quad L^\infty(0, T; L^2(\Omega)),$$

$$\frac{du_k}{dt} \to \frac{du}{dt} \quad \text{weakly in } \quad L^2(0, T; (H^r(\Omega))^*),$$

$$Z_k \to Z \quad \text{weakly}^* \text{ in } \quad L^\infty(\Omega \times (0, T); \mathbb{R}^2),$$

$$|\nabla u_k|^{p-2}\nabla u_k \to |\nabla u|^{p-2}\nabla u \quad \text{weakly in } \quad L^{\frac{p}{p-1}}(\Omega \times [0, T]; \mathbb{R}^2)$$

Owing to the Aubin-Lions-Simon lemma [17], without loss of generality we may assume that $u_k \to u$ in $C\left([0, T]; [W^{1,2}(\Omega)]^*\right)$. See [18], we know that $h(\nabla G_\sigma * u_k) \to h(\nabla G_\sigma * u)$ uniformly on $C\left(\bar{\Omega} \times [0, T]\right)$.

Therefore,

$$\int_0^{t_*}\int_\Omega (1 - h(\nabla G_\sigma * u_k))Z_k \cdot \nabla w dx dt \to \int_0^{t_*}\int_\Omega ((1 - h(\nabla G_\sigma * u))Z \cdot \nabla w dx dt \ .$$

$$\int_0^{t_*}\int_\Omega h(\nabla G_\sigma * u_k)|\nabla u_k|^{p-2}\nabla u_k \cdot \nabla w dx dt \to \int_0^{t_*}\int_\Omega h(\nabla G_\sigma * u)|\nabla u|^{p-2}\nabla u \cdot \nabla w dx dt$$

$$\int_0^{t_*}\int_\Omega (1 - h(\nabla G_\sigma * u))|\nabla u| dx dt \le \lim_{k\to+\infty} \inf \int_0^{t_*}\int_\Omega (1 - h(\nabla G_\sigma * u_k))|\nabla u_k| dx dt.$$

$$\int_0^{t_*}\int_\Omega h(\nabla G_\sigma * u)|\nabla u|^p dx dt \le \lim_{k\to+\infty} \inf \int_0^{t_*}\int_\Omega h(\nabla G_\sigma * u_k)|\nabla u_k|^p dx dt$$

The first term of (31) is lower-semicontinuous (see [21]), we have

$$\|u(t_*) - w(t_*)\|^2 \le \lim_{k\to+\infty} \inf \|u_k(t_*) - w(t_*)\|^2.$$

The remaining terms of (31) are either linear, or constants, or of order $O(\epsilon_k)$, Hence, in the limit we get

$$\begin{aligned}
&\|u(t_*) - w(t_*)\|^2 + 2\int_0^{t_*}\int_\Omega \frac{dw}{dt} u dx dt \\
&\quad + 2\int_0^{t_*}\int_\Omega h(\nabla G_\sigma * u)|\nabla u|^p dx dt + 2\mu\int_0^{t_*}\int_\Omega (1 - h(\nabla G_\sigma * u))|\nabla u| dx dt \\
&\le \|u_0 - w(0)\|^2 + \|w(t_*)\|^2 - \|w(0)\|^2 + 2\int_0^{t_*}\int_\Omega h(\nabla G_\sigma * u)|\nabla u)|^{p-2}\nabla u \cdot \nabla w dx dt \\
&\quad + 2\mu\int_0^{t_*}\int_\Omega (1 - h(\nabla G_\sigma * u))\, Z \cdot \nabla w dx dt;
\end{aligned}$$

Passing to the limit in (30), we obtain (11). When $t_* = T$, (u, Z) satisfies (8), (11) and (12). Finally, by density, the test function v and w in (11) and (12) can be take from the space indicated in Definition 1.

3 Experimental results

In what follows, we provide some experimental results using our model in image restoration. The discretized version of the the PDE (7) is utilized out using standard finite difference scheme via additive operator splitting (AOS) [22].

A discrete m-dimensional image can be regarded as a vector $f \in \mathbb{R}^N$, whose components $f_i (i = 1, \cdots, N)$, display the grey values at the pixels. Pixel i represents location x_i . Let h_l denote the grid size in the l direction. We consider discrete times $t_k := k\tau$, where $k \in \mathbb{N}$ and τ is the time step size. By u_i^k and $\mathcal{C}_i^k$ we denote approximations to $u(x_i, t_k)$ and $h(\nabla G_\sigma * u(x_i, t_k))|\nabla u(x_i, t_k)|^{p-2} + \mu(1 - h(\nabla G_\sigma * u(x_i, t_k)) \frac{1}{|\nabla u(x_i, t_k)|}$, respectively, where the gradient is replaced by central differences.

The simplest discretization of (7) with reflecting boundary conditions is given by

$$\frac{u_i^{k+1} - u_i^k}{\tau} = \sum_{l=1}^{m} \sum_{j \in \mathcal{N}_l(i)} \frac{\mathcal{C}_j^k + \mathcal{C}_i^k}{2h_l^2} \left(u_j^{k+1} - u_i^{k+1} \right)$$

where $N_l(i)$ consists of the two neighbors of pixel i along the l direction (boundary pixels may have only one neighbor). In vector matrix notation this becomes

$$\frac{u^{k+1} - u^k}{\tau} = \sum_{l=1}^{m} A_l(u^k) u^{k+1}$$

where $A_l(u^k) = [a_{ij}^l(u^k)]$ with

$$a_{ij}^l(u^k) := \begin{cases} \frac{\mathcal{C}_i^k + \mathcal{C}_j^k}{2h_l^2}, & j \in \mathcal{N}_l(i), \\ -\sum\limits_{n \in \mathcal{N}_l(i)} \frac{\mathcal{C}_i^k + \mathcal{C}_n^k}{2h_l^2}, & j = i, \\ 0, & \text{otherwise.} \end{cases}$$

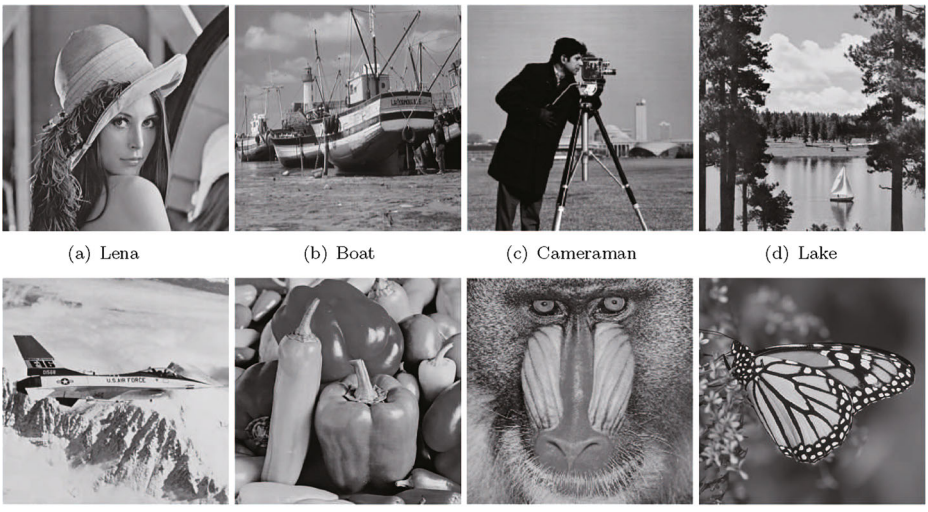

Fig. 1 Test images used in Table 1

Table 1 Comparative quantitative results of algorithms for several images. Noise are AWGN with standard deviation 20 and 30

Images	σ	PM[14]	TV[16]	Chen[8]	Li[12]	Zhou[24]	AFBD[18] (p=1.5)	AFBD[18] (p=1)	Proposed
Lena	20	30.32	31.17	31.20	31.35	31.05	30.71	31.35	**31.56**
		0.9085	0.9165	0.9167	0.9163	0.9006	0.9001	0.9145	**0.9251**
	30	28.27	29.51	29.45	29.64	29.40	29.15	29.68	**29.88**
		0.8634	0.8793	0.8784	0.8817	0.8613	0.8524	0.8793	**0.8941**
Boat	20	28.87	29.29	29.04	29.17	29.23	28.92	29.31	**29.42**
		0.8919	0.8970	0.8950	0.8979	0.8862	0.8811	0.8961	**0.9062**
	30	26.79	27.54	27.41	27.53	27.43	27.22	27.58	**27.74**
		0.8325	0.8468	0.8443	0.8501	0.8321	0.8258	0.8447	**0.8591**
Cameraman	20	30.47	31.59	31.62	31.64	31.50	31.33	31.86	**32.14**
		0.8987	0.9094	0.9118	0.9068	0.8923	0.8863	0.9123	**0.9217**
	30	27.92	29.30	29.48	29.38	29.41	29.03	29.49	**29.87**
		0.8432	0.8533	0.8666	0.8641	0.8392	0.8183	0.8665	**0.8796**
Lake	20	28.64	29.23	29.14	29.24	29.11	28.98	29.28	**29.46**
		0.8982	0.9107	0.9163	0.9189	0.9024	0.8939	0.9168	**0.9266**
	30	26.64	27.51	27.37	27.52	27.39	27.25	27.54	**27.77**
		0.8658	0.8729	0.8779	0.8845	0.8584	0.8505	0.8804	**0.8949**
Starfish	20	28.02	28.42	27.91	28.20	28.35	28.23	28.55	**28.78**
		0.8422	0.8454	0.8431	0.8505	0.8396	0.8386	0.8491	**0.8565**
	30	25.73	26.32	26.04	26.32	26.32	26.26	26.43	**26.67**
		0.7697	0.7916	0.7834	0.7993	0.7852	0.7826	0.7961	**0.8055**
Airplane	20	30.37	31.32	31.17	31.31	31.03	30.76	31.42	**31.81**
		0.9168	0.9224	0.9233	0.9247	0.8997	0.8962	0.9262	**0.9343**
	30	28.18	29.36	29.24	29.47	29.11	28.89	29.60	**29.87**
		0.8812	0.8890	0.8891	0.8984	0.8555	0.8459	0.8980	**0.9124**
Peppers	20	30.65	31.50	31.56	31.62	31.42	30.29	31.01	**31.71**
		0.9225	0.9281	0.9297	0.9307	0.9181	0.9056	0.9275	**0.9344**
	30	28.54	29.78	29.72	29.88	29.75	28.57	29.34	**30.05**
		0.8859	0.8964	0.8954	0.9020	0.8863	0.8709	0.9006	**0.9092**
Baboon	20	27.19	27.60	27.35	27.64	27.59	28.06	27.82	**28.20**
		0.8920	0.8943	0.8951	0.9026	0.8926	0.8956	0.8973	**0.9049**
	30	25.03	25.69	25.45	25.71	25.62	26.08	25.87	**26.09**
		0.8173	0.8276	0.8267	0.8362	0.8240	0.8299	0.8330	**0.8394**
Monarch	20	30.65	31.26	31.39	31.46	30.95	30.12	31.54	**32.03**
		0.9434	0.9502	0.9478	0.9516	0.9196	0.9006	0.9536	**0.9630**
	30	28.22	29.04	29.36	29.49	28.86	28.04	29.46	**30.04**
		0.9144	0.9237	0.9197	0.9285	0.8911	0.8549	0.9279	**0.9465**
Parrot	20	28.46	28.68	28.56	28.65	28.63	27.73	28.72	**28.92**
		0.8197	0.8316	0.8381	0.8387	0.8156	0.8105	0.8357	**0.8461**
	30	26.16	26.41	26.73	26.69	26.47	25.85	26.62	**26.92**
		0.7573	0.7787	0.7897	0.7960	0.7657	0.7342	0.7857	**0.8018**

The measurements are PSNR(first),and MSSIM(second). The bold values denote the best performance

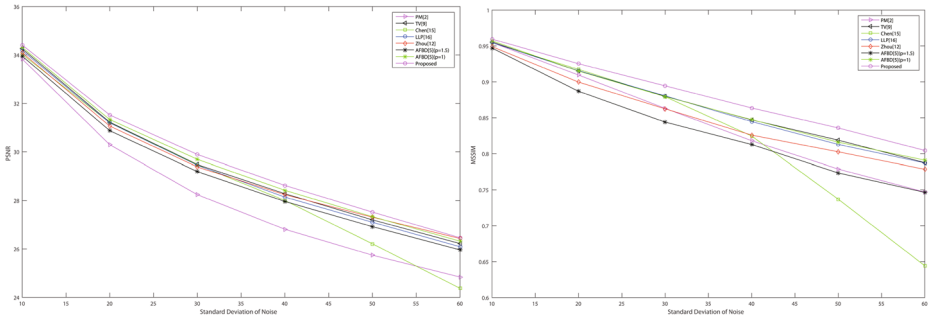

Fig. 2 PSNR representation as a function of noise standard deviation. Input image is Lena polluted by AWGN

The additive operator splitting (AOS) [22] scheme is given by

$$u^{k+1} = \frac{1}{m}\sum_{l=1}^{m}(I - m\tau A_l(u^k))^{-1}u^k$$

Fig. 3 Qualitative comparative results for algorithms. Input image is Lena corrupted by AWGN with standard deviation 20. Zoomed part of Lena is shown for better visual comparison

The operators $B_l(u^k) = I - m\tau A_l(u^k)$ describe one-dimensional diffusion processes along the x_l axes. Under a consecutive pixel numbering along the direction l they come down to strictly diagonally dominant tridiagonal matrices which can be efficiently inverted by the Thomas algorithm, see [22] for more details.

To compare the restoration results quantitatively, we use two error measures including peak signal-to-noise ratio (PSNR) and mean structural similarity (MSSIM), which are widely used in the image processing literature. In all these measurements, the greater number indicates better denoising performance. All the experiments are performed under Matlab R2014b with AMD FX-7500 CPU at 2.1GHz and 8 GB RAM.

For the sake of verifying the effectiveness of our proposed method for image denoising, some experiments are practiced to compare the denoising result of the proposed method with that of the other methods: PM [14] ($c(s) = \frac{1}{1+(s/K)^2}$), TV [16] ((2) with $p = 1$), Chen et al. [8], Liet al. [12], Zhou et al. [24] and AFBD [18].

In all the experiments in this paper, the time step is set as 0.2. The stopping time was chosen so that the best PSNR is obtained. In PM [14], the threshold K is calculated using Canny noise estimator [5]: $K = 0.9 \times mean(|\nabla u|)$. We fix $p = 1.5, k = 0.02$ and $\mu = \frac{1}{3}$ for

Fig. 4 Qualitative comparative results for algorithms. Input image is Cameraman corrupted by AWGN with standard deviation 20. Zoomed part of Cameraman is shown for better visual comparison

our proposed model. The Gaussian convolution in our model is carried out by the discrete version with rotationally symmetric Gaussian lowpass filter of size 5×5 with variance 0.8.

Figure 1 shows the test images used in our experiments. The quantitative results presented in Table 1 compare the proposed method with some state-of-the-art methods using PSNR and MSSIM for 10 images illustrated in Fig. 1. The test images in this table are contaminated by AWGN with standard derivation 20 and 30. This table confirms that the proposed method has the highest PSNR and MSSIM in all cases. The comparisons of PSNR values with the comparative techniques on the image Lena are plotted in Fig. 2. We see that the proposed method always yields the highest PSNR in all noise levels.

Figures 3, 4, 5 make a qualitative comparison among the several denoising algorithms. Figure 3 makes a visual comparison among the denoising methods in zoomed part of Lena image. As can be seen in this figure, in PM [14] the edges are sharp while image suffers from isolated points and staircase effect. TV [16], Chen [8], Zhou [24] and AFBD [18] ($p = 1$) yield staircase effect. Image of AFBD [18] ($p = 1.5$) is blurry and contains many of noise

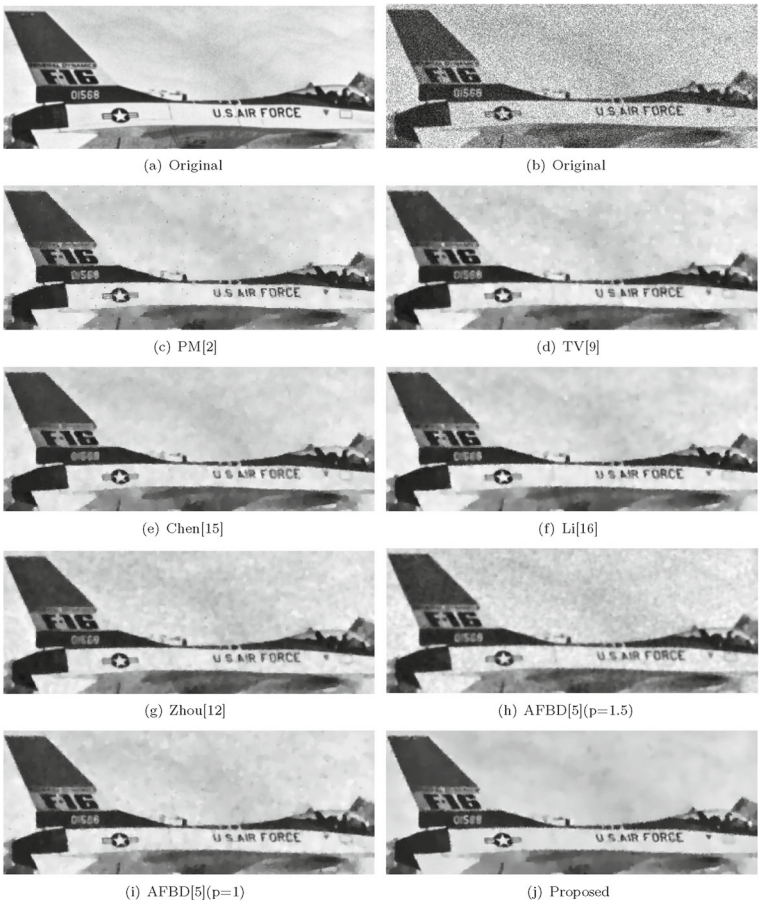

(a) Original (b) Original

(c) PM[2] (d) TV[9]

(e) Chen[15] (f) Li[16]

(g) Zhou[12] (h) AFBD[5](p=1.5)

(i) AFBD[5](p=1) (j) Proposed

Fig. 5 Qualitative comparative results for algorithms. Input image is Airplane corrupted by AWGN with standard deviation 25. Zoomed part of Airplane is shown for better visual comparison

components. The staircasing and blurring effects of Li [12] are more than the proposed method. Based on the results, the proposed method has the best visual quality.

Figure 4 shows a zoomed part of Cameraman image. PM [14] causes isolated points. TV [16] and Chen [8] cause staircase effect. The edges in Zhou [24] are sharper than AFBD [18] ($p = 1.5$), but both blur the image. The filtered images by Li [12] and AFBD [18] ($p = 1$) yield a little staircase effect. The proposed method removes noise while preserving the feature of image.

Figure 5 compares the methods for zoomed part of Airplane image. The edges in PM [14] are sharp, but it still suffers from isolated points. Chen [8] and Li [12] blur the images. Many noise components remain in Zhou [24] and AFBD [18] ($p = 1.5$). TV [16] and AFBD [18] ($p = 1$) still suffer from staircase effect. The proposed method outperforms other methods in term of feature preservation and improved noise reduction, see, in particular, the number region of the Airplane is much better preserved in our proposed method compared to other methods.

4 Conclusion

In this paper, we introduced an adaptive second-order PDE model which can preserve edge and alleviate the staircase effect while removing the noise. By utilizing a combination TV diffusion and p-Laplacian term an edge preserving image smoothing method is obtained. The existence of a weak solution of the proposed model was investigated. Experimental results show that the proposed method provides superior visual quality than the compared models and gets better signal-to-noise ratio and mean structural similarity with noise-free images for the final denoised images. Images expanded using our model are natural looking.

References

1. Andreu F, Mazn JM, Caselles V (2001) The Dirichelt Peroblem for the total varitaion flow. J Funct Anal 180(2):347–403. https://doi.org/10.1007/978-3-0348-7928-6_5
2. Andreu F, Caselles V, Diaz JI, Marzon JM (2002) Some qualitative properties for the total variation flow. J Funct Anal 188(2):516–547. https://doi.org/10.1006/jfan.2001.3829
3. Aubert G, Kornprobst P (2006) Mathematical problems in image processing: partial difierential equations and the calculus of variations, 2nd. Springer, New York
4. Blomgren P, Chan TF, Mulet P, Wong CK (1997) Total variation image restoration: numerical methods and extensions. Int Conf Image Process 3:384–387. https://doi.org/10.1109/ICIP.1997.632128
5. Canny J (1986) A Computational Approach to Edge Detection. IEEE Trans Pattern Anal Mach Intell 8(6):679–698. https://doi.org/10.1109/TPAMI.1986.4767851
6. Chambolle A, Lions PL (1997) Image recovery via total varition minimization and related problems. Numerische Mathematik 76(2):167–188. https://doi.org/10.1007/s002110050258
7. Chan TF, Esedoglu S, Park FE (2007) Image decomposition combining staircase reduction and texture extraction. J Vis Commun Image Represent 18(6):464–486. https://doi.org/10.1016/j.jvcir.2006.12.004
8. Chen Y, Levine S, Rao M (2006) Variable exponent, linear growth functionals in image restoration. Siam J Appl Math 66(4):1383–1406. https://doi.org/10.1137/050624522
9. Gilboa G, Sochen N, Zeevi YY (2004) Image enhancement and denoising by complex diffusion processes. IEEE Trans Pattern Anal Mach Intell 26(8):1020–1036. https://doi.org/10.1109/TPAMI.2004.47
10. Guidotti P, Longo K (2011) Two enhanced fourth-order diffusion models for image denoising. J Math Imaging Vision 40(2):188–198. https://doi.org/10.1007/s10851-010-0256-9

11. Kuijper A (2007) P-Laplacian Driven Image Processing. IEEE Int Conf Image Process 5:257–260. https://doi.org/10.1109/ICIP.2007.4379814
12. Li F, Li Z, Pi L (2010) Variable exponent functionals in image restoration. Appl Math Comput 216(3):870–882. https://doi.org/10.1016/j.amc.2010.01.094
13. Lysaker M, Lundervold A, Tai X (2003) Noise removal using forth-order partial difffential equation with applications to medical magnetic resonance images in space and time. IEEE Trans Image Process 12(12):1579–1590. https://doi.org/10.1109/TIP.2003.819229
14. Perona P, Malik J (1990) Scale-space and edge detection using anisotropic diffucsion. IEEE Trans Pattern Anal Mach Intell 12(7):629–639. https://doi.org/10.1109/34.56205
15. Rafsanjani HK, Sedaaghi MH, Saryazdi S (2016) Efficient diffusion coefficient for image denoising. Comput Math Appl 72(4):893–903. https://doi.org/10.1016/j.camwa.2016.06.005
16. Rudin L, Osher S, Fatemi E (1992) Nonlinear total variation based noise removal algorithms. Physica D 60(1-4):259–268. https://doi.org/10.1016/0167-2789(92)90242-F
17. Simon J (1986) Compact sets in the space $L^p(0, T; B)$. Annali di Matematica 146(1):65–96. https://doi.org/10.1007/BF01762360
18. Suray Prasath VB, Urbano JM, Vorotnikov DA (2015) Analysis of adaptive forward-backward diffusion flows with applications in image processing. Inverse Prob 31(10):105008. https://doi.org/10.1088/0266-5611/31/10/105008
19. Suray Prasath VB, Vorotnikov DA, Pelapur R, Jose S, Seetharaman G, Palaniappan K (2015) Multiscale Tikhonov-Total variation image restoration using spatially varying edge coherence exponent. IEEE Trans Image Process 24(12):5220–5235. https://doi.org/10.1109/TIP.2015.2479471
20. Temam R (1979) Navier-stokes equuations. Studies in Mathematics and its Applications, vol 2. North-Holland Publishing Co., Amsterdam
21. Vorotnikov D (2012) Global generalized solutions for Maxwell-alpha and Euler-alpha equations. Nonlinearity 25(2):309–327. https://doi.org/10.1088/0951-7715/25/2/309
22. Weickert J, Romeny BH, Viergever MA (1998) Efficient and reliable schemes for nonlinear diffusion filtering. IEEE Trans Image Process 7(3):398–410. https://doi.org/10.1109/83.661190
23. You YL, Kaveh M (2000) Fourth-order partial differential equations for noise removal. IEEE Trans Image Process 9(10):1723–1730. https://doi.org/10.1109/83.869184
24. Zhou B, Mu CL, Feng J, Wei W (2012) Continuous level anisotropic diffusion for noise removal. Appl Math Model 36(8):3779–3786. https://doi.org/10.1016/j.apm.2011.11.026
25. Zvyagin VG, Vorontnikov DA (2008) Topological approximation methods for evoluctionary problems of nonlinear hydrodynamics. De Gruyter Series in Nonliear Analysis and Applications, vol 12, De Gruyter & Co., Berlin

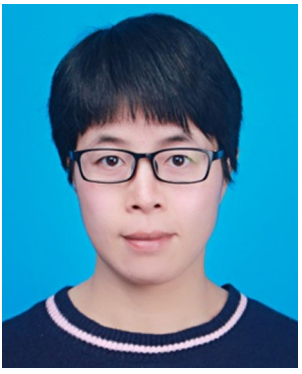

Xiaojuan Zhang received the MSc degree in computational mathematics from Xiamen University, China, in 2004. She is currently pursuing the PhD degree form department of mathematics of Shanghai University, China. Her current research interests include image processing and partial differential equations.

Wanzhou Ye received the MSc degree in 1994, the PhD degree in 2001, from Nankai University, both in math, He is with the department of mathematics of Shanghai University, where he is now a professor. His current research interests include wavelets analysis, image processing and compressed sensing.